The evolution of antiherbivore defenses and their contribution to species coexistence in the tropical tree genus *Inga*

Thomas A. Kursar[a,b,1], Kyle G. Dexter[c], John Lokvam[a], R. Toby Pennington[d], James E. Richardson[d], Marjorie G. Weber[a], Eric T. Murakami[a], Camilla Drake[d], Ruth McGregor[d], and Phyllis D. Coley[a,b]

[a]Department of Biology, University of Utah, Salt Lake City, UT 84112; [b]Smithsonian Tropical Research Institute, Box 0843-03092, Balboa, Panama; [c]Laboratoire Evolution et Diversité Biologique, Unité Mixte de Recherche 5174, Centre National de la Recherche Scientifique, Université Paul Sabatier, Bâtiment 4R3, 31062 Toulouse, France; and [d]Royal Botanic Garden, Edinburgh EH3 5LR, United Kingdom

Edited by Anurag A. Agrawal, Cornell University, Ithaca, NY, and accepted by the Editorial Board July 27, 2009 (received for review May 1, 2009)

Plants and their herbivores constitute more than half of the organisms in tropical forests. Therefore, a better understanding of the evolution of plant defenses against their herbivores may be central for our understanding of tropical biodiversity. Here, we address the evolution of antiherbivore defenses and their possible contribution to coexistence in the Neotropical tree genus *Inga* (Fabaceae). *Inga* has >300 species, has radiated recently, and is frequently one of the most diverse and abundant genera at a given site. For 37 species from Panama and Peru we characterized developmental, ant, and chemical defenses against herbivores. We found extensive variation in defenses, but little evidence of phylogenetic signal. Furthermore, in a multivariate analysis, developmental, ant, and chemical defenses varied independently (were orthogonal) and appear to have evolved independently of each other. Our results are consistent with strong selection for divergent defensive traits, presumably mediated by herbivores. In an analysis of community assembly, we found that *Inga* species co-occurring as neighbors are more different in antiherbivore defenses than random, suggesting that possessing a rare defense phenotype increases fitness. These results imply that interactions with herbivores may be an important axis of niche differentiation that permits the coexistence of many species of *Inga* within a single site. Interactions between plants and their herbivores likely play a key role in the generation and maintenance of the conspicuously high plant diversity in the tropics.

plant defenses | community assembly | phylogenetic signal | herbivory | tropical diversity

Because plants and herbivores constitute more than half of the macroscopic diversity on Earth, their interactions play a fundamental role in biodiversity and ecosystem function. Two central issues are how defenses against herbivores have evolved and how such variation in defenses among species might regulate plant community composition (1–6). Here, we use a phylogenetic approach to investigate the diversification of antiherbivore defenses and their role in community assembly.

Several paradigms dominate our understanding of plant/herbivore macroevolution. Ehrlich and Raven (7) observed that related plants host similar herbivores and suggested that plant–herbivore coevolution is driven by changes in plant secondary metabolites. Their hypothesis predicts that more closely related species should have more similar chemistry (8, 9). An alternative hypothesis is that natural selection caused by herbivores may result in rapid trait evolution such that closely related species have divergent defenses. Another distinct, and widely accepted, proposition suggests that species coexisting at a single site are likely to differ in key ecological niche dimensions (10, 11).

Here, we examine the diversity of antiherbivores defenses, their phylogenetic signal, and their contribution to species coexistence in the tree genus *Inga* (Fabaceae: Mimosoideae). *Inga* diversified rapidly during the last 2 million to 10 million years and now has >300 species distributed throughout the Neotropics (12, 13). Furthermore, *Inga* is one of the most species-rich and abundant genera in local communities (14) with 43 species comprising 6.0% of the stems recorded from 25 ha in Ecuador (15). In 50 ha in Panama, *Inga* comprises 7% of all tree species (16).

We measured antiherbivore defenses in *Inga* for 12 species in Panama and 31 species in Peru (six species are shared). We focused our study on the defenses of young, expanding leaves because their rate of damage is ≈100-fold higher than for mature leaves and they receive >80% of the damage accrued throughout the lifetime of a leaf (17, 18). During the very short period (1–3 weeks) of leaf expansion in the *Inga* study species, 25% of the leaf area was eaten in Panama and 37% was eaten in Peru (Fig. 1*A*). Therefore, we argue that the defense traits under the strongest natural selection are those of young leaves. Chemical defenses are likely important for young leaves as *Inga* species invest up to 50% dry weight (DW) of young leaves in secondary metabolites (19). Young leaves are also defended against herbivory through developmental defenses such as rapid leaf expansion or delayed chloroplast development (20–23). Finally, *Inga* leaves have extrafloral nectaries that produce nectar and attract leaf-defending ants only during leaf expansion (Fig. 1*B* and refs. 24–26). Thus, we measured the following defensive traits on young leaves: the presence or absence of chemical compounds from classes that are relevant to antiherbivore defense, the rate of leaf expansion, chloroplast development (chlorophyll content), and the average number of ants per extrafloral nectary.

The primary goal of this study is to determine how interspecific variation in defenses may contribute to our understanding of the origin and maintenance of tropical diversity. Therefore, we also constructed a phylogenetic hypothesis for all of the focal species by using plastid DNA sequence data. We also assessed coexistence in the field by using data on the abundance and richness of *Inga* from the 50-ha forest dynamics plot in Panama and a network of tree plots in southern Peru. These data allowed

Author contributions: T.A.K., K.G.D., J.L., R.T.P., and P.D.C. designed research; T.A.K., K.G.D., J.L., R.T.P., J.E.R., M.G.W., E.T.M., C.D., R.M., and P.D.C. performed research; K.G.D., J.L., R.T.P., J.E.R., and P.D.C. analyzed data; and T.A.K., K.G.D., J.L., R.T.P., and P.D.C. wrote the paper.

The authors declare no conflict of interest.

This article is a PNAS Direct Submission. A.A.A. is a guest editor invited by the Editorial Board.

Data deposition: The sequences reported in this paper have been deposited in the GenBank database (accession nos. FJ974145, FJ974151, FJ974164, FJ974180, FJ974241, FJ974279, FJ974351, FJ974409, FJ974438, FJ974449, FJ974509, FJ974628, FJ974673, FJ974683, FJ974713, FJ974870, FJ974883, FJ974910, FJ974975, FJ974988, FJ975003, FJ975011, FJ975039, GQ118709–GQ118890, GQ871263–GQ871278, and GQ892055).

[1]To whom correspondence should be addressed. E-mail: kursar@biology.utah.edu.

This article contains supporting information online at www.pnas.org/cgi/content/full/0904786106/DCSupplemental.

Fig. 1. Young leaves of *I. poeppigiana* being damaged by a hemipteran (*Left*; photo by Robyn Burnham) and young leaves of *I. thibaudiana* with extrafloral nectaries being visited by the ant *Ectatomma* (*Right*; photo by Tania Brenes-Arguedes).

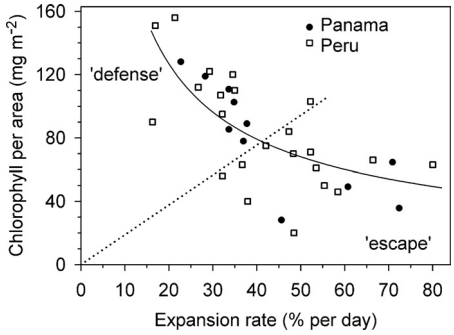

Fig. 2. The rate of expansion of young leaves expressed as the percentage increase in area per day (% per day) versus the chlorophyll content (mg·m^{-2}) for *Inga* species from Panama (n = 11) and Peru (n = 23). For all species combined, there is a significant negative relationship [exp = 971 × (chl$^{-0.68}$); r^2 = 0.50, $P < 0.0001$]. The dotted diagonal line separates species into two equal-sized groups designated as defense and escape.

us to test the above-mentioned hypotheses that pertain to defense evolution (7–9) and community assembly (10, 11) by asking whether or not (*i*) defense traits are phylogenetically conserved and (*ii*) coexisting species differ more in defense strategies than would be expected by chance.

Results and Discussion

Chemical defenses vary considerably among *Inga* species and include compounds belonging to several distinct classes that are known for their antiherbivore effects (27). Secondary metabolites include phenolics, saponins and nonprotein amino/imino acids, and an overexpressed protein amino acid, tyrosine (28–30). Twelve types of metabolites were identified that arise from branch points in the shikimic acid, phenylpropanoid and flavonoid pathways (Fig. S1; referred to as "phenolics"). These include quinic, gallic, and cinnamic acid derivatives and tyrosine and tyramine, either in pure or conjugated form. The most common and widespread phenolics were the flavan-3-ols, the polymeric forms of which are called condensed tannins.

Thirty-two species contained one or more forms of phenolic metabolite; 12 species contained saponins. In all, the 37 study species were distributed among 13 distinct chemotypes, each a unique combination of phenolics and saponins (Table S1). The most common chemotype, polymers of the flavan-3-ol, gallocatechin-epigallocatechin gallate, was shared by 11 species. In addition to *Inga*, this class of metabolites is known from at least two genera of mimosoid legumes *Stryphnodendron* (31) and *Cojoba* (Table S2), which suggests that it may be the ancestral chemical defense in the genus. All other chemotypes were considerably less common: nine of the 13 chemotypes were represented by only one or two species (Table S1).

Eleven species from Panama were also examined for protein/nonprotein amino/imino acid content, a class characteristic of legumes (32). There were 17 different compounds (Table S1), 11 of which are derived from five different amino acid precursors (33), with the remainder being uncharacterized. No two species had the same suite of compounds.

The rate of leaf expansion, a key developmental defense, determines how long a leaf is tender and vulnerable to herbivores. This rate varied widely among species, ranging from 16% to 80% per day (Fig. 2), equivalent to the variation among all non-*Inga* species sampled (34, 35). The chlorophyll content of young leaves also varied (Fig. 2), with some species having almost white young leaves (20 mg·m^{-2}) and others with normal greening (156 mg·m^{-2}). There was a significant negative relationship between expansion and chlorophyll within *Inga* (Fig. 2), which was true for each site independently (Panama, r^2 = 0.71, $P <$ 0.001; Peru, r^2 = 0.41, $P < 0.001$) and all species together (r^2 = 0.50, $P < 0.001$).

To test whether the correlations between expansion and chlorophyll could be caused by convergence, we examined their phylogenetically independent contrasts (PICs) (36). There was a significant negative correlation between PICs for the two traits (across 200 randomly selected Bayesian trees: $\bar{r}^2$ = 0.37, $\bar{P}$ = 0.0001, $P < 0.05$ for 99% of trees). We have argued that this widespread tradeoff may be caused by an unavoidable physiological constraint that restricts simultaneous allocation of resources to both rapid expansion and the costly photosynthetic system (21–23). A second, although not mutually exclusive, explanation is that this association could arise because of pleiotropic effects.

Ant abundance, a biotic defense, also varied among *Inga* species. Ant visitation to the extrafloral nectaries of young leaves differed 20-fold among species and on average was 2.3 times higher in Peru compared with Panama (t test, $P < 0.001$; Fig. S2). We tested the hypothesis that ant visitation could be associated with developmental defenses. Using nonphylogenetic regressions and PICs, we found no significant correlation between expansion rates and ant visitation (r^2 = 0.01, P = 0.72, Fig. S2; PICs: $\bar{r}^2$ = 0.01, $\bar{P}$ = 0.48) or between chlorophyll and ant visitation (r^2 = 0.01, P = 0.51; PICs: $\bar{r}^2$ = 0.01, $\bar{P}$ = 0.45).

The chemical, nectary, and leaf-development traits discussed above vary considerably among species. The broad distribution of traits seen in *Inga* could result from two quite distinct evolutionary trajectories. The species with dissimilar defenses could be the most phylogenetically distant (high phylogenetic signal), a pattern consistent with Ehrlich and Raven's (7) view of plant–herbivore macroevolution. Alternatively, close relatives may have divergent defenses (low phylogenetic signal), an unexpected pattern that would suggest distinct macroevolutionary processes.

Are More Closely Related Species More Similar in Their Defenses? The assumption that more closely related species have similar defenses has dominated coevolutionary theory (7). However, within the genus *Inga*, we inferred that defense strategy shows little phylogenetic signal. Our phylogenetic hypothesis for *Inga* species, based on ≈6,000 bp of plastid DNA sequence and inferred by using Bayesian approaches, resolves several clades with strong support (posterior probabilities ≥95%; Fig. 3). This phylogenetic tree shows more resolution than that of Richardson et al. (13), who sampled fewer *Inga* species and used only ≈1,500 bp of DNA sequence.

We quantified the chemical distances between species based

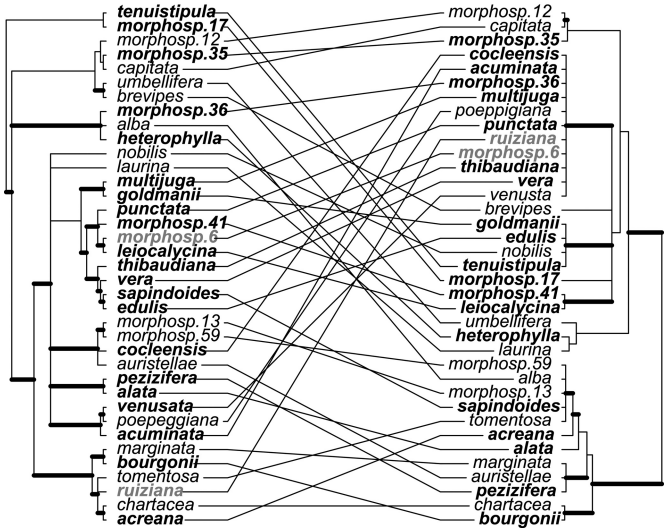

Fig. 3. Phylogenetic tree (*Left*; 50% majority rule consensus tree from Bayesian analysis of 6,000 bps of plastid DNA) and chemistry dendrogram (*Right*) for *Inga* species. Thickened branches on the phylogeny represent >0.95 posterior probability for the adjacent node. The chemistry dendrogram was generated by using hierarchical clustering of presence/absence data for 13 defense chemicals (phenolics and saponins, weighted equally). Thickened branches are adjacent to nodes with $P < 0.1$ according to multiscale bootstrapping analysis (approximately >90% bootstrap support; see *SI Text*). Species in bold are classified as defense (see Fig. 2), and other species are classified as escape. Gray species are unclassified because of lack of data.

on the number of compounds for which species differed (see *Materials and Methods*). We found a weak correlation between phylogenetic distance and chemical distance between species, based on combining data on saponin and phenolic compounds and weighting them equally (Mantel Tests across 200 Bayesian trees, $\bar{r} = 0.13$, $\bar{P} = 0.041$, $P < 0.05$ for 70% of trees; Fig. S3). The weak phylogenetic signal for total chemical distance derives from moderate similarity in phenolic chemistry of closely related species (Mantel Tests, $\bar{r} = 0.23$, $\bar{P} = 0.021$, $P < 0.05$ for 95% of trees). There was no relationship between phylogenetic distance and saponin chemical distance (Mantel Tests, $\bar{r} = 0.03$, $\bar{P} = 0.31$), and for Panamanian species, there was no relationship between phylogenetic and amino/imino acid chemical distances (Mantel Tests, $\bar{r} = -0.04$, $\bar{P} = 0.51$).

We also compared the phylogeny with a dendrogram of the chemical similarities among species of *Inga* (Fig. 3). Inspection of Fig. 3 showed weak congruence. Some closely related species (*I. capitata*, *I.* morphosp.12 and *I.* morphosp.35) shared similar chemistry, but more frequently, close relatives were chemically dissimilar. For example, the clade containing *I. umbellifera*, *I. brevipes*, *I.* morphosp.36, and *I. heterophylla* exhibited chemical profiles that spanned the entire chemical space. For the five species having only saponins, two, *I.* morphosp.59 and *I.* morphosp.13, are sister in the phylogeny, whereas the other three species, *I. alba*, *I. sapindoides*, and *I. tomentosa*, are placed in three other clades. We conclude that, for *Inga*, related species are more divergent in their secondary metabolite composition than expected by chance.

To test for a phylogenetic signal for developmental and ant defenses, we first conducted a principal component analysis (PCA) to determine the orthogonality of these two proposed defense strategies. The first axis was highly correlated with expansion rate and chlorophyll content (development), whereas the second axis was highly correlated with ant visitation rates. The first axis showed significant phylogenetic signal (Blomberg's K across 200 Bayesian trees: $\bar{K} = 0.69$, $\bar{P} = 0.04$, $P < 0.05$ for 73% of trees) (37), although still lower than the expected value of one under pure Brownian evolution. The second axis showed no detectable phylogenetic signal ($\bar{K} = 0.42$, $\bar{P} = 0.87$). To further visualize the evolution of these characters, we classified species into the conventional categories of "escape" vs. "defense" (35) based on species' coordinates in Fig. 2 and as having high vs. low ant visitation. These binary characters showed no detectable phylogenetic signal when mapped onto 100 Bayesian trees sampled at stationarity (Fig. S4) (ref. 38 and http://mesquiteproject.org). We also show in Fig. 3 how species were classified with respect to escape vs. defense. Hence, we found a significant phylogenetic signal only for developmental traits and only in the case when we treated these defenses as quantitative traits and analyzed them by PCA.

We also assessed Mantel correlations of the chemical distances between species with the differences between species in the values along each of the two principal component axes representing developmental and ant defense. Neither was correlated with chemistry (first axis: Mantel $r = -0.03$, $P = 0.49$; second axis: Mantel $r = -0.01$, $P = 0.85$). These results and the PCAs suggest that developmental, ant, and chemical profiles are independent defensive strategies that also have evolved independently of one another. Species in the cotton clade also showed independent evolution of ant and chemical defenses (39).

We have sampled only 37 species of *Inga*, and further sampling could result in subclades showing more uniformity in defensive strategies. However, that is unlikely for several reasons. First, our sampling spans the taxonomic diversity of the genus, representing 9 of 14 sections recognized by Pennington (12). Second, some of the species included are definitively shown to be closely related but chemically divergent. For example, two species pairs show a profound lack of sequence divergence in the rapidly evolving plastid regions we have used. These are *I. goldmanii* and *I. multijuga*, identical for ≈6,000 bp of plastid DNA, and *I. leiocalycina* and *I. morphosp.6*, differing by two substitutions in 6,000 bp; and they nevertheless show contrasting chemical defenses (Fig. 3).

Although there is a significant association of developmental defense strategy with phylogeny, we find little evidence for phylogenetic signal in the other, independent defense traits, ants, and chemistry. Our data show both extensive variation in defense traits and considerable differences among close relatives, a pattern that is consistent with defense strategies in *Inga* being evolutionarily labile (40). This finding contrasts with the prevailing hypothesis [Ehrlich and Raven (7)], which implies that closely related plant species should be similar in defense strategies. Few studies have examined defenses across many related species, although terpenes in the genus *Bursera* (Burseraceae) showed low congruence between a chemical dendrogram and a phylogeny (3).

Coexistence and Defense Trait Similarity. Could antiherbivore defenses be an important mechanism of niche partitioning in community assembly? To address this question, we assessed phylogenetic and defense trait dispersion in *Inga* communities. We used the inverse of the metrics of Webb (41) so that positive values represent overdispersion and negative values represent underdispersion. In the 50-ha forest dynamics plot in Panama, we found that co-occurring *Inga* species are more distantly related than expected by chance (overdispersion; Fig. 4; across 200 Bayesian trees, two-tailed t tests: $\bar{\text{NRI}} = 0.68$, $\bar{t} = 15.83$, $\bar{P} < 0.00001$, $P < 0.05$ for 100% of trees; $\bar{\text{NTI}} = 0.50$, $\bar{t} = 7.83$, $\bar{P} = 0.005$, $P < 0.05$ for 99% trees). In contrast, in Peru we found phylogenetic underdispersion of *Inga* communities (Fig. 4; two-tailed t tests: $\bar{\text{NRI}} = -0.66$, $\bar{t} = -5.08$, $\bar{P} < 0.0002$, $P < 0.05$ for 100% of trees; $\bar{\text{NTI}} = -0.50$, $\bar{t} = -3.15$, $\bar{P} = 0.021$, $P < 0.05$ for 91% trees). This site difference likely reflects the different spatial and environmental scales that were sampled. In Panama,

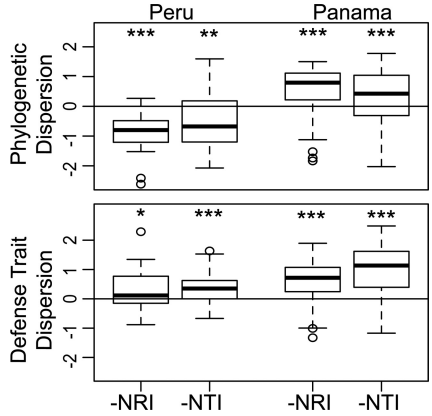

Fig. 4. Phylogenetic and defense trait dispersion for *Inga* communities in Peru and Panama. Phylogenetic results are for one, randomly selected Bayesian tree. Values given are the inverse of the net relatedness index (NRI) and nearest taxon index (NTI) following Webb (41). Values > 0 indicate overdispersion, and values < 0 indicate underdispersion. The departure of communities from the null expectation (zero) of communities being randomly assembled was evaluated by using two-sided *t* tests for phylogenetic dispersion and one-sided *t* tests for defense trait dispersion (*, $P < 0.05$; **, $P < 0.01$; ***, $P < 0.001$).

we assessed co-occurrence within the homogenous habitat of the 50-ha plot (local spatial scale). In Peru, we sampled across a 150-×-200-km area (regional spatial scale) and in two different habitat types, terra firme and floodplain forest (42). We suggest that a phylogenetic signal for traits associated with habitat preference (cf. ref. 41) may underlie the contrasting phylogenetic structures.

At both spatial scales, including Peru where neighbors were close relatives, the co-occurring species were more dissimilar than expected at random for a defense index combining the developmental, ant, and chemical traits (see *Materials and Methods*; Fig. 4; Peru: one-tailed *t* test: $\bar{\text{N}}\text{RI} = 0.32, t = 2.26, P = 0.016$; $\bar{\text{N}}\text{TI} = 0.40, t = 3.56, P = 0.0007$; Panama: one-tailed *t* test: $\bar{\text{N}}\text{RI} = 0.60, t = 13.75, P < 0.00001$; $\bar{\text{N}}\text{TI} = 1.06, t = 17.35, P < 0.00001$). We also assessed the dispersion of two leaf traits that are likely unrelated to herbivore defense, the presence vs. absence of wings on the rachis and the number of leaflets per leaf. We found no evidence for overdispersion of leaf traits in Panama (one-tailed *t* test: $\bar{\text{N}}\text{RI} = -0.68, t = -8.96, P < 0.00001$; $\bar{\text{N}}\text{TI} = -0.05, t = -0.74, P = 0.46$) or Peru ($\bar{\text{N}}\text{RI} = 0.29, t = 1.33, P = 0.196$; $\bar{\text{N}}\text{TI} = -0.04, t = -0.16, P = 0.87$).

These results illustrate that, although nondefense traits such as leaflet number and presence of wings are randomly or underdispersed, defensive traits at both sites are overdispersed. Divergence in chemical defenses at single sites has also been shown for another speciose tree genus, *Bursera* (4). The co-occurrence of species having divergent defense strategies could be caused by herbivores preferentially foraging on individuals with common defense phenotypes. By such a mechanism, herbivores may structure the assembly of rainforest tree communities.

Conclusions

Our analysis of defenses is consistent with the idea that, in *Inga*, the arms race between plants and their herbivores has led to rapid and divergent trait evolution. The young leaves of *Inga* make substantial investments in chemical defenses [up to 50% of DW (19)] and developmental defenses and extrafloral nectar, suggesting that herbivory is a strong selective agent. The chemical, biotic, and developmental defenses of young leaves showed considerable variation among species. The observations of Ehrlich and Raven (7) suggest that defenses evolve by small changes (8, 9) and low trait divergence also might be predicted from the recent radiation of *Inga* (13). Instead we found a weak or no correlation of phylogeny with defensive traits. These results suggest divergent selection on, and rapid evolution of, antiherbivore defenses in *Inga* (40) and thus are consistent with the recognized importance of the interactions between hosts and natural enemies in driving diversifying evolution in both plants and animals (43).

We also argue that divergent defenses could be a principal mechanism structuring community assembly. Most species of *Inga* are restricted to similar habitats and may vary little in resource use; they also have similar flower and fruit morphologies (12), thus suggesting similar pollinator and dispersal syndromes. Therefore, the high number of species of *Inga*, up to 43, that coexist at a single site (15) presents an enigma. We found that, regardless of whether the co-occurring species of *Inga* are less related (Panama) or more closely related (Peru) than expected by chance, the assemblage of *Inga* at a single site differs more in defense strategy than random. In addition, most lepidopteran herbivores specialize on a subset of the species of *Inga* present at a given site (44). Therefore, for *Inga* species, high local abundance and diversity may be caused by antagonistic, density-dependent interactions with these specialized natural enemies. Thus, niche differentiation may occur via differences in antiherbivore defenses, rather than differences in resource use, pollination, or dispersal.

Are there parallels with other genera? A striking pattern in the tropics is the disproportionate contribution to total diversity made by genera having 100 or more species, such as *Eugenia*, *Miconia*, *Piper*, *Pouteria*, and *Psychotri*a. Many such genera also have high local abundance and diversity (14–16). For example, in 25 ha in Ecuador 10.7% of the species, 17% of the basal area, and 17% of the stems are contributed by only three genera (15). In most speciose genera, as with *Inga*, the congeners appear to have similar functional morphologies, reproductive syndromes and habitat preferences, raising yet again the enigmatic issue of coexistence. Perhaps interactions with natural enemies will be key to understanding the maintenance of diversity in the tropics.

It also is unclear what ecological processes have driven speciation in the large genera typical of tropical rainforests. We argue that *Inga*'s radiation seems unlikely to result from adapting to differences in the abiotic environment, pollinators, or seed dispersers. Instead, we suggest that the *Inga* radiation was driven by interactions with natural enemies (6) through the diversification of antiherbivore defenses. Thus, although links between herbivore pressure and host speciation in tropical forests are tentative, our hypothesis for rapid, divergent selection on antiherbivore defenses also may explain the radiations in *Inga* and other large genera in the tropics (6).

Materials and Methods

Study Sites. Data were collected in Panama and Peru. Barro Colorado Island (BCI) is a field station administered by the Smithsonian Tropical Research Institute in the Republic of Panama (9° N, 79° W). The average total yearly rainfall is 2,600 mm, 90% of which falls during the rainy season from May through December, and the average daily temperature is 27 °C. The vegetation is moist-lowland forest (45). We used 0.25-ha subplots of the 50-ha forest dynamics plot on BCI to provide *Inga* community composition data for Panama (46). The second field site was at Los Amigos Biological Station in Peru and is operated by the Amazon Conservation Association (13° S, 70° W). The site is ≈250 m above mean sea level, receives 2,600 mm of rainfall annually, and averages 24 °C. The forest is lowland rainforest and encompasses terra firme (upland) forest and seasonally flooded forest. We used a network of 0.25-ha *Inga* plots across the department of Madre de Dios (in which Los Amigos is located and where two surveys were located) to provide community composition data for Peru (42). We worked on the most common *Inga* species present at each site. We collected data on 12 species from Panama and 31 from Peru. Six species occurred in both Panama and Peru, based on similar morphology and DNA sequences. *I. laurina*, *I. nobilis*, *I. ruiziana*, and *I. sapindoides* had

similar secondary metabolite profiles, whereas the secondary metabolites of *I. marginata* and *I. umbellifera*, although similar, were not identical between sites.

Sample Collection. Ecological and defense trait data were taken for young leaves on understory saplings. Rates of young-leaf expansion were calculated as the percentage increase in area per day for leaves between 20% and 80% of full size. The number of ants visiting extrafloral nectaries of young leaves was counted (number of ants per nectary) during censuses along trails between 10 AM and 3 PM. Chlorophyll content ($mg \cdot m^{-2}$) was determined for young leaves estimated to be between 60% and 80% of full size. See *SI Text* for detailed methods and Table S3 for species values.

Chemical Analyses. Leaves collected for chemical analysis were processed and stored on site in Peru and Panama before shipment to Utah (see *SI Text* for details). An *Inga*-specific fractionation protocol (Fig. S5) developed in the lab at the University of Utah produced seven chemically distinct (19, 47) fractions: lipids, phenolics, saponins, amino acids, organic acids, proteins, and the insoluble parts of the cell walls (marc). Two of these, phenolics and saponins, either have been shown to account for the great majority of the deterrent activity in *Inga* extracts (19, 47) or are presumed to be deterrent based on their mass abundance and the literature (27). The phenolic fraction, when present, was analyzed in detail for chemical content. Analysis was by HPLC with detection by photo-diode array (for UV-absorbing metabolites) and evaporative light-scattering (ELS) or electrospray ionization (ESI) MS. Based on earlier work with *Inga* defense chemistry (19, 28–30, 47), we were in many cases able to identify whole classes of compounds (e.g., catechin/epicatechin polymers) solely by their UV absorption and mass spectra. Where this was not possible, the structures of unknowns were solved explicitly by NMR and high-resolution MS (28–30, 47). For a complete description of phenolic chemical structures, see Fig. S1. Each species was classified according to chemotypes that were based on the class of phenolic metabolite and the presence/absence of saponins when either one or both were present. If either phenolics or saponins was 5% or less of the total active fraction (as estimated by ELS detection), it was omitted from the analysis. Ten species from Panama were analyzed by HPLC-ESI-MS for protein/nonprotein amino/imino acid content. Metabolites having primary or secondary amines were first derivatized (48). Tertiary amines were analyzed directly. One other Panama species, *I. laurina*, was analyzed by gas chromatography after derivatization (49). Several individuals from each species were analyzed separately and, in all cases, chemical profiles based on presence/absence of compounds were identical within a species.

Phylogenetic Reconstruction. Samples for DNA were dried in silica gel, and sterile and fertile herbarium vouchers were identified by using the taxonomic monograph of *Inga* (12) and verified by its author T.D. Pennington (Royal Botanic Gardens, Kew; Table S4). Total genomic DNA extraction followed Richardson et al. (13). Six plastid DNA regions were sequenced: *trn*LF (50), *trn*D-T (47, 51) and additional internal sequencing primers designed for this study: *psb*A-*trn*H (52, 53), *rps*16 (54), *rpo*C1 (55), and *ndh*F-*rpl*32 (56). All primer sequences plus PCR and sequencing protocols are in *SI Text*.

Bayesian analysis was performed by using MrBayes 3.1.1 (57) with 5,000,000 generations of four simultaneous MCMC chains, sampling one tree every 10,000 generations. MrModelTest 3.7 (58) was used to select the best-fitting substitution model for each plastid region. Phylogenetic trees were rooted by using outgroup sequences from *Zygia*, which is shown to be most closely related to *Inga* in phylogenetic analyses using multiple genera from tribe Ingeae.

We assessed correlations between expansion rate, chlorophyll content, and ant visitation by using linear regressions and PICs (36). We evaluated chemical distances between species as the number of compounds for which species have a different state (presence vs. absence), standardized by the maximum observed distance. We assessed the correlation between chemical and phylogenetic distance by using Mantel tests. The chemistry dendrogram (Fig. 3) was constructed by using hierarchical clustering (59). We conducted a PCA on continuous trait data to derive independent axes of defense trait variation. We evaluated phylogenetic signal for the first two axes (the two axes that showed eigenvalues >1) by using analyses of Blomberg's K (37). We evaluated a possible evolutionary relationship between chemical defense strategy and these axes by using a Mantel test relating chemical distance to differences between species along the first two axes.

We evaluated the distance between species in defense traits as the average of distances for the different chemical classes and for distances between species in escape/defense (developmental) strategy and ant visitation rates. We standardized each chemical or other defense class or axis to vary from 0 and 1, such that each was weighted equally in the total defense trait analyses. We evaluated the distance between species in leaf traits (wings and leaflet number) as the average distance between species along two axes derived from a principal component analysis of the leaf traits. All analyses were conducted in the R statistical environment (R Core Development Team 2009), and details can be found in *SI Text*.

ACKNOWLEDGMENTS. We thank E. Leigh for stimulating discussions and O. Acevedo and B. Jimenez for moral and logistical support at the Smithsonian Tropical Research Institute; K. Rudolph, K. Bromberg, D. Dvorett, S. Ring, B. Wolfe, and M.-J. Epps for field assistance in Panama; N. Pitman for intellectual input and J. Saldaña, C. Lazo, and F. Para for field work in Peru; officials from Autoridad Nacional del Ambiente of Panama and Instituto Nacional de Recursos Naturales of Peru for permission to conduct field work; S. Lee and D. Grapov for assistance with the chemical characterizations at the University of Utah; officials at the Center for Tropical Forest Science of the Smithsonian Tropical Research Institute for use of the data from the 50-ha plot (http://ctfs.si.edu/datasets/bci); and M. Lavin, M. Lemes, M. Hollingsworth, and A. Clark for phylogenetic research. K.G.D. was supported by National Science Foundation Grant DDIG-0608368 and grants from the Amazon Conservation Association, American Philosophical Society, Duke University, Explorer's Club, Society for Systematic Biology, and Sigma Xi. T.A.K. and P.D.C. were supported by National Science Foundation Grants DEB-0234936 and DEB-0640630 and Research Experience for Undergraduate supplements. R.T.P. was supported by Leverhulme Trust Study Abroad Fellowship RF/2/2006/0142.

1. Agrawal AA (2007) Macroevolution of plant defense strategies. *Trends Ecol Evol* 22:103–109.
2. Agrawal AA, Fishbein M (2006) Plant defense syndromes. *Ecology* 87:S132–S149.
3. Becerra JX (1997) Insects on plants: Macroevolutionary chemical trends in host use. *Science* 276:253–256.
4. Becerra JX (2007) The impact of herbivore–plant coevolution on plant community structure. *Proc Natl Acad Sci USA* 104:7483–7488.
5. Farrell BD, Dussourd DE, Mitter C (1991) Escalation of plant defense: Do latex and resin canals spur plant diversification? *Am Nat* 138:881–900.
6. Schemske DW (2002) in *Foundations of Tropical Forest Biology: Classic Papers with Commentaries*, eds Chazdon RL, Whitmore TC (Univ Chicago Press, Chicago), pp 163–173.
7. Ehrlich PR, Raven PH (1964) Butterflies and plants: A study in plant coevolution. *Evolution* (Lawrence, Kans) 18:586–608.
8. Berenbaum MR, Feeny P (1981) Toxicity of angular furanocoumarins to swallowtail butterflies: Escalation in a coevolutionary arms race? *Science* 212:927–929.
9. Berenbaum MR, Zangerl AR (1998) Chemical phenotype matching between a plant and its insect herbivore. *Proc Natl Acad Sci USA* 95:13743–13748.
10. Cavender-Bares J, Ackerly DD, Baum DA, Bazzaz FA (2004) Phylogenetic overdispersion in Floridian oak communities. *Am Nat* 163:823–843.
11. Webb CO, Gilbert GS, Donoghue MJ (2006) Phylodiversity-dependent seed mortality, size structure, and disease in a Bornean rain forest. *Ecology* 87:S123–S131.
12. Pennington TD (1997) *The Genus Inga* (Royal Botanic Gardens, London).
13. Richardson JE, Pennington RT, Pennington TD, Hollingsworth PM (2001) Rapid diversification of a species-rich genus of neotropical rain forest trees. *Science* 293:2242–2245.
14. Valencia R, Balslev H, Miño GP (1994) High tree α diversity in Amazonian Ecuador. *Biodiver Conserv* 3:21–28.
15. Valencia R, et al. (2004) in *Tropical Forest Diversity and Dynamism: Findings from a Large-Scale Plot Network*, eds Losos EC, Leigh EG, Jr (Univ Chicago Press, Chicago), pp 609–628.
16. Hubbell SP, Foster RB, Condit R, Lao S, Perez R (1995) *Demographic Tree Data from the 50-ha Barro Colorado Island Forest Dynamics Plot, 1982–1995* (Smithsonian Institution, Washington, DC), CTFS Forest Dynamic Plot Data Series, CD-ROM.
17. Brenes-Arguedas T, et al. (2006) Contrasting mechanisms of secondary metabolite accumulation during leaf development in two tropical tree species with different leaf expansion strategies. *Oecologia* 149:91–100.
18. Coley PD, Aide TM (1991) in *Plant-Animal Interactions: Evolutionary Ecology in Tropical and Temperate Regions*, eds Price PW, Lewinsohn TM, Fernandes WW, Benson WW (Wiley, New York), pp 25–49.
19. Lokvam J, Kursar TA (2005) Divergence in structure and function of young leaf chemical defenses in two co-occurring *Inga* species. *J Chem Ecol* 31:2563–2580.
20. Kursar TA, Coley PD (1991) Nitrogen content and expansion rate of young leaves of rainforest species: Implications for herbivory. *Biotropica* 123:141–150.
21. Kursar TA, Coley PD (1992) Delayed development of the photosynthetic apparatus in tropical rainforest species. *Func Ecol* 6:411–422.
22. Kursar TA, Coley PD (1992) The consequences of delayed greening during leaf development for light absorption and ligh use efficiency. *Plant Cell Environ* 15:901–909.
23. Kursar TA, Coley PD (1992) Delayed greening in tropical leaves: An antiherbivore defense? *Biotropica* 24:256–262.
24. Brenes-Arguedas T, Coley PD, Kursar TA (2008) Divergence in the chemical ecology of *Inga* between two neotropical sites. *J Ecol* 96:127–135.

25. Koptur S (1984) Experimental evidence for defense of *Inga* (Mimosoideae) saplings by ants. *Ecology* 65:1787–1793.
26. Koptur S (1985) Alternative defenses against herbivores in *Inga* (Fabaceae: Mimosoideae) over an elevational gradient. *Ecology* 66:1639–1650.
27. Seigler DS (1998) *Plant Secondary Metabolism* (Kluwer, Boston).
28. Lokvam J, Brenes-Arguedas T, Lee JS, Coley PD, Kursar TA (2006) Allelochemic function for a primary metabolite: The case of L-tyrosine hyper-production in *Inga umbellifera* (Fabaceae). *Am J Bot* 93:1109–1115.
29. Lokvam J, Clausen TP, Grapov D, Coley PD, Kursar TA (2007) Galloyl depsides of tyrosine from young leaves of *Inga laurina*. *J Nat Prod* 70:134–136.
30. Lokvam J, Coley PD, Kursar TA (2004) Cinnamoyl glucosides of catechin and dimeric procyanidins from young leaves of *Inga umbellifera* (Fabaceae). *Phytochemistry* 65:351–358.
31. Palazzo de Mello J, Petereit F, Nahrstedt A (1996) Flavan-3-ols and prodelphinidins from *Stryphnodendron adstringens*. *Phytochemistry* 41:807–813.
32. Wink M (2003) Evolution of secondary metabolites from an ecological and molecular phylogenetic perspective. *Phytochemistry* 64:3–19.
33. Romeo JT (1998) Functional multiplicity among nonprotein amino acids in Mimosoid legumes: A case against redundancy. *Ecoscience* 5:287–294.
34. Coley PD, Kursar TA (1996) in *Tropical Forest Plant Ecophysiology*, eds Mulkey SS, Chazdon R, Smith AP (Chapman & Hall, New York), pp 305–336.
35. Kursar TA, Coley PD (2003) Convergence in defense syndromes of young leaves in tropical rainforests. *Biochem Syst Ecol* 21:929–949.
36. Garland T, Harvey PH, Ives AR (1992) Procedures for the analysis of comparative data using phylogenetically independent contrasts. *Syst Biol* 41:18–32.
37. Blomberg SP, Garland T, Jr, Ives AR (2003) Testing for phylogenetic signal in comparative data: Behavioral traits are more labile. *Evolution (Lawrence, Kans)* 57:717–745.
38. Maddison W, Maddison D (2007) *Mesquite: A Modular System for Evolutionary Analysis* (Mesquite Software, Austin, TX), version 2.01.
39. Rudgers JA, Strauss SY, Wendel JE (2004) Tradeoffs among antiherbivore resistance traits: Insights from Gossypieae (Malvaceae). *Am J Bot* 91:871–880.
40. Revell LJ, Harmon LJ, Collar DC (2008) Phylogenetic signal, evolutionary process, and rate. *Syst Biol* 57:591–601.
41. Webb CO (2000) Exploring the phylogenetic structure of ecological communities: an example for rain forest trees. *Am Nat* 156:145–155.
42. Dexter KG (2008) The effects of dispersal on macroecological patterns. PhD Thesis. (Duke University, Durham, NC).
43. Brockhurst MA (2007) Ecology: Death and destruction determine diversity. *Curr Biol* 17:R512–R514.
44. Kursar TA, Wolfe BT, Epps MJ, Coley PD (2006) Food quality, competition, and parasitism influence feeding preference in a neotropical lepidopteran. *Ecology* 87:3058–3069.
45. Leigh EG (1999) *Tropical Forest Ecology: A View from Barro Colorado Island* (Oxford Univ Press, New York).
46. Hubbell SP, Condit R, Foster RB (2005) *Barro Colorado Forest Census Plot Data* (Smithsonian Tropical Research Institute, Panama).
47. Coley PD, et al. (2004) Divergent defensive strategies of young leaves in two neotropical species of *Inga*. *Ecology* 86:2633–2643.
48. Tapuhi Y, Schmidt DE, Lindner W, Karger BL (1981) Dansylation of amino acids for high-performance liquid chromatography analysis. *Anal Biochem* 115:123–129.
49. Stalling DL, Gehrke CW, Zumwalt RW (1968) A new silylation reagent for amino acids bis(trimethylsilyl)trifluoroacetamide (BSTFA). *Biochem Biophys Res Commun* 31:616–622.
50. Taberlet P, Gielly L, Pautou G, Bouvet J (1991) Universal primers for amplification of three noncoding regions of chloroplast DNA. *Plant Mol Biol* 17:1105–1109.
51. Grivet D, Heinze B, Vendramin GG, Petit RJ (2001) Genome walking with consensus primers: Application to the large single copy region of chloroplast DNA. *Mol Ecol Notes* 1:345–349.
52. Sang T, Crawford DJ, Stuessy TF (1997) Chloroplast DNA phylogeny, reticulate evolution, and biogeography of *Paeonia* (Paeoniaceae). *Am J Bot* 84:1120–1136.
53. Tate JA, Simpson BB (2003) Paraphyly of *Tarasa* (Malvaceae) and diverse origins of the polyploid species. *Syst Bot* 28:723–737.
54. Oxelman B, Liden M, Berglund D (1997) Chloroplast *rps*16 intron phylogeny of the tribe *Sileneae* (Caryophyllaceae). *Plant Syst Evol* 206:393–410.
55. Hollingsworth ML, et al. (2009) Selecting barcoding loci for plants: Evaluation of seven candidate loci with species-level sampling in three divergent groups of land plants. *Mol Ecol Res* 9:439–457.
56. Shaw J, Lickey EB, Schilling EE, Small RL (2007) Comparison of whole chloroplast genome sequences to choose noncoding regions for phylogenetic studies in angiosperms: The tortoise and the hare III. *Am J Bot* 94:275–288.
57. Huelsenbeck JP, Ronquist F (2001) MRBAYES: Bayesian inference of phylogenetic trees. *Bioinformatics* 17:754–755.
58. Posada D, Crandall KA (2001) Selecting the best-fit model of nucleotide substitution. *Syst Biol* 50:580–601.
59. Everitt BS, Landau S, Leese M (2001) *Cluster Analysis* (Taylor & Francis, Florence, KY), 4th Ed.

Supporting Information

Kursar et al. 10.1073/pnas.0904786106

SI Text

Sample Collection. Ecological data were taken for young leaves on saplings (0.5–2.5 m tall) growing in the understory. More than 50 km of trails were walked regularly to search for plants with young leaves. Panamanian collections were made from March 2001 to November 2004, and Peruvian collections were made from May to December 2007.

Rates of leaf expansion were determined by measuring the area of marked leaves every 1–3 days throughout expansion. Expansion rates were calculated as the percentage increase in area per day for leaves between 20% and 80% of full size. Because of herbivore damage, many leaves had to be excluded so expansion data were based on an average of 13 individual leaves per species. Because temperatures differed by 3.9 °C between the study sites/seasons, we adjusted expansion rates from Peru by a factor of 1.51, equivalent to a Q_{10} of 2.7 that we have measured for respiration in tropical leaves. The number of ants visiting extrafloral nectaries of young leaves was counted (# nectary^{-1}) during censuses along trails between 10 AM and 3 PM for an average of 83 plants per species. Chlorophyll content (mg·m^{-2}) was determined for an average of nine young leaves per species estimated to be between 60% and 80% of full size. A known area of leaf tissue was homogenized in 95% ethanol and centrifuged, and absorbances at 663 and 725 nm were measured with a portable spectrophotometer (Milton Roy, Spectronic Mini 20). See Table S3 for values and sample sizes averaged by species.

Chemical Analyses. Young leaves were collected from understory saplings and were between 10% and 90% of full expansion. Less than 1/3 of the leaves on a single flush were collected to minimize negative impacts to the plant. For each species, leaves were collected from many different plants and stored separately. Most of the leaves collected in Panama were homogenized in 95% ethanol by using a Polytron (Brinkmann Instruments) and then stored at −50 °C until shipped to Utah for analysis. Some samples from Panama and all leaves collected in Peru were dried under vacuum (<1 Torr in Panama or 10 Torr, with silica gel, in Peru) for 36–48 h and then stored at −50 °C in Panama and −15 °C in Peru in doubly sealed plastic bags with silica gel until being shipped to Utah. Extracts of young leaves from 37 *Inga* species from Panama and Peru were analyzed for phenolic and saponin content. Panamanian samples were also analyzed for nonprotein amino acids.

Phylogenetic Reconstruction. PCR and sequencing protocols for trnD-T are given in ref. 1. The psbA-trnH region was amplified and sequenced with primers psbA GTTATGCATGAACGTAATGCTC and trnH CGCGCATGGTGGATTCAAATCC. The rps16 regions was amplified and sequenced with primers rps16-F GTGGTAGAAAGCAACGTGCGA and rps16-R TCGGGATCGAACATCAATTGCAAC. PCR conditions for psbA-trnH and rps16 were: one cycle of 94 °C for 2 min; 30 cycles of 94 °C for 1 min, 50 °C for 1 min, and 72 °C for 1 min; one cycle of 72 °C for 10 min. The trnL-F region was amplified and sequenced in two parts by using primer pairs trnL c CGAAATCGGTAGACGCTACG, trnL d GGGGATAGAGGGACTTGAAC, and trnL e GGTTCAAGTCCCTCTATCCC, trnL f ATTTGAACTGGTGACACGAG. PCR conditions for trnL-F were: one cycle of 94 °C for 4 min; 35 cycles of 94 °C for 45 s, 55 °C for 45 s, and 72 °C for 3 min; one cycle of 72 °C for 10 min. The ndhF-rpl32 region was amplified and sequenced following Shaw et al. (2), and rpoC1 was amplified and sequenced following Hollingsworth et al. (3). For the ≈50% of samples that did not produce PCR products for ndhF-rpl32 using Shaw et al. (2) protocols, we developed new primers (forward: GGAGCTGCCATTCCAAAAT; reverse: TTCGCCAATTTTATCTCTTTTG) and new PCR conditions: one cycle of 94 °C for 2 min; 30 cycles of 95 °C for 1 min, 48 °C for 1 min, 65 °C for 4 min with ramp of 0.3/s to 65 °C; one cycle of 65 °C for 5 min. For psbA-trnH, rps16, rpoCI, ndhF-rpl32 and trnL-F, the 25-μL reaction mix consisted of 16.1 μL of H_2O, 2.5 μL of *Taq* buffer, 2.5 μL of dNTP mix (10 mM concentration for each nucleotide), 0.75 μL of each primer (10 μM concentration), 1.25 μL of $MgCl_2$ (50 mM concentration), 0.125 μL of *Taq* polymerase (0.625 units), and 1 μL of DNA template. In some cases of nonamplification, 2 μL of DNA template was used (with the volume of H_2O adjusted accordingly. Cleaned PCR products were sequenced by using ABI capillary sequencers (Applied Biosystems) at the University of Edinburgh and Northwoods DNA. Sequences were assembled by using Sequencher v4.5 (Gene Codes) and aligned manually, which was unproblematic given low sequence divergence.

Bayesian analysis was performed by using MrBayes 3.1.1 (4) with 5,000,000 generations of four simultaneous MCMC chains, sampling one tree every 10,000 generations. ModelTest 3.7 (5) was used to select the best-fitting substitution model for each plastid region. Phylogenetic trees were rooted by using outgroup sequences from *Zygia*, which is shown to be most closely related to *Inga* in phylogenetic analyses by using multiple genera from tribe Ingeae.

We ran initial analyses using all accessions from both Peru and Panama. Because in all cases accessions of species found in both Peru and Panama were resolved as monophyletic, or nearly so, we reduced each to a single accession so as not to bias analyses attempting to detect phylogenetic signal.

For subsequent ecological analyses that involved phylogenies, we randomly selected 100 or 200 after burn-in phylogenetic trees from the Bayesian phylogenetic analysis. All trees were made ultrametric before subsequent analyses by using nonparametric rate smoothing (6) in the APE package (7) of the R statistical environment (R Core Development Team 2009). All analyses were also conducted by using a set of 173 equally parsimonious trees and gave equivalent results.

Relationships Among Defense Traits. We evaluated relationships between expansion rate, chlorophyll content, and ant visitation for all species by using conventional least-squares linear regression and linear models with PICs and forcing the intercept through zero (8). For analyses that involved all species, trait values were averaged between Peru and Panama for shared species. Analyses were conducted in the R statistical environment (R Core Development Team 2009). We report r^2 values adjusted for sample size and parameter number. PICs were obtained by using the APE package in R. For the ant visitation character, differences among species in visitation rates were compared by using data that were normalized for each site because ant abundance was >2 times higher in Peru.

Chemical Defense Similarity. We evaluated chemical dissimilarity (or distance) between species as the total number of compounds for which they differed in presence/absence state, standardized by the maximum value for this metric across all species pairs (thus, distance varies from 0 to 1). We first calculated dissimilarity separately for phenolics and saponins. To obtain the total

chemical distance between species, we combined the phenolics and saponins data and upweighted saponins such that the maximum distance for saponins would be equal to the maximum distance for phenolics. For BCI Inga, we also calculated the chemical distance for nonprotein amino acid composition. We evaluated the correlation between chemical distances and phylogenetic distance (across the 200 Bayesian trees) by using Mantel tests (9).

We constructed a dendrogram for the chemical composition data by using hierarchical clustering (10) of the equally weighted phenolics and saponins data. We assessed support for the dendrogram by using multiscale bootstrapping and calculating the approximately unbiased P values for nodes with the pvclust package (11) in R.

Evolutionary Lability in Escape vs. Defense and Ant Visitation. Because the above analyses indicated that expansion rate and chlorophyll content covaried strongly, we used a PCA to derive independent axes of defense trait variation for variables for which we had continuous data (expansion rate, chlorophyll content, and ant visitation). The PCA produced two axes with eigenvalues >1. The first axis was highly correlated with expansion rate ($r = -0.71$) and chlorophyll content ($r = 0.70$), whereas the second axis was highly correlated with ant visitation ($r = 0.98$).

We assessed whether there was significant phylogenetic signal for these two defense axes by determining whether Blomberg's K (12) was significantly different from 0, based on 999 randomizations of the data (across 200 Bayesian trees; using the R package Picante; http://picante.r-forge.r-project.org).

We were lacking expansion rate or chlorophyll content data for 1/3 of the species in Peru. To include these species in analyses, we derived a binary characterization, which represented the two extremes of the developmental defense syndrome. For species with chlorophyll and expansion data, species were classified as escape vs. defense (13) based on where the species were placed on a plot of expansion rate by chlorophyll content (see Fig. 2). For most of the remaining species where data were incomplete, T.A.K. and P.D.C. classified them as escape or defense by using their extensive field experience with visually estimating chlorophyll content (Table S3).

We assessed phylogenetic signal for this escape/defense character by optimizing the character under a maximum parsimony criterion onto the 50% majority rule Bayesian consensus tree by using Mesquite version 2.01 (Fig. S4 and ref. 14). To account for topological uncertainty, the procedure "Trace over Trees" was used to summarize ancestral state reconstructions >100 Bayesian trees sampled at stationarity. To test whether phylogenetic distribution of escape/defense was significantly different from random the number of parsimony steps in these characters was measured across 100 Bayesian trees sampled at stationarity was compared with: (*i*) the number of steps in the same characters optimized on to 1,000 random trees produced in MacClade 4.08 (15) and (*ii*) the number of steps in the same characters when the states were randomized among terminal taxa using the "reshuffle character" option in Mesquite (14). We used a similar approach to visualize the evolution of a binary character representing ant visitation rates (high vs. low visitation; Fig. S4).

We also determined whether developmental and ant defense axes (axes 1 and 2, respectively, from PCA analyses above) were orthogonal to chemical defenses. We first obtained distance matrices for these axes by calculating the Euclidean distance between species for each axis. We then used Mantel tests to assess whether there was a significant correlation between each distance matrix and the chemical distance matrix.

Community Phylogenetic and Defense Trait Dispersion. We evaluated the phylogenetic and defense trait structure of Inga communities by using the inverse of the NRI and NTI of Webb (16) and as calculated following Kembel and Hubbell (17). We conducted analyses separately for Panama and Peru and only used species from each location when randomly drawing species for null communities. We shuffled tip labels in the phylogeny (18) to generate null communities for calculating the normalized metrics NRI and NTI. There was no significant phylogenetic signal for abundance in Peru or Panama (across 200 Bayesian trees; Peru: $\bar{K} = 0.64$, $\bar{P} = 0.36$; Panama: $\bar{K} = 0.96$, $\bar{P} = 0.12$), although lack of significance may be caused by low sample size, particularly in Panama.

We calculated a defense distance matrix between species separately for Peru and Panama by averaging the distance matrices for the different chemical classes above (the nonprotein amino acid matrix being present for Panama only) with an ant visitation rate distance matrix (absolute distance between species in ant visitation rate, standardized by the maximum value) and an escape vs. defense distance matrix (where matrix cells have a binary state of 1 if the two species differ in this classification and 0 if they are the same). Thus, the different chemical defense classes, ant visitation rate, and escape vs. defense were all weighted equally. We obtained a bio-neighbor joining tree from the total defense distance matrix and treated this as a phylogenetic tree to evaluate whether there was a signal for abundance in the defense data. There was not (Peru: $K = 0.12$, $P = 0.85$; Panama: $K = 0.59$, $P = 0.62$), and we therefore shuffled species labels in the defense distance matrix to generate null communities for defense trait structure analyses.

We evaluated whether the distribution of NRI and NTI values for communities were significantly different from zero by using t tests following Kembel and Hubbell (17). All phylogenetic and defense trait structure analyses were conducted by using functions in the Picante and APE packages in R (http://picante.r-forge.r-project.org).

We also conducted defense community structure analyses by using the first two axes from the PCA above to represent developmental and ant defense trait variation. Specifically, we averaged the chemical distance matrices with a distance matrix derived from the Euclidean distance between species along the first two principal component axes. This necessarily resulted in a loss of sample size, with regard to species, for Peru because many species were lacking expansion and chlorophyll data. This analysis gave results in the same direction as the above analyses (Panama: $\tilde{\text{NRI}} = 0.48$, $t = 8.74$, $P < 0.00001$; $\tilde{\text{NTI}} = 0.59$, $t = 10.53$, $P < 0.00001$; Peru: $\tilde{\text{NRI}} = 0.08$, $t = 0.34$, $P = 0.370$; $\tilde{\text{NTI}} = 0.24$, $t = 1.36$, $P = 0.092$).

To determine whether other traits, not related to herbivore defense, showed a similar pattern of community structure, we obtained data for each species on the presence of wings on the leaf rachis and the number of leaflets per leaf (Table S3). We created a distance matrix for calculation of NRI and NTI values by averaging distance matrices for the first two axes from a PCA of these characters.

1. Dexter KG (2008) The effects of dispersal on macroecological patterns. PhD Thesis (Duke University, Durham, NC).
2. Shaw J, Lickey EB, Schilling EE, Small RL (2007) Comparison of whole chloroplast genome sequences to choose noncoding regions for phylogenetic studies in angiosperms: The tortoise and the hare III. *Am J Bot* 94:275–288.
3. Hollingsworth ML, et al. (2009) Selecting barcoding loci for plants: Evaluation of seven candidate loci with species-level sampling in three divergent groups of land plants. *Mol Ecol Res* 9:439–457.
4. Huelsenbeck JP, Ronquist F (2001) MRBAYES: Bayesian inference of phylogenetic trees. *Bioinformatics* 17:754–755.
5. Posada D, Crandall KA (1998) MODELTEST: Testing the model of DNA substitution. *Bioinformatics* 14:817–818.

6. Sanderson MJ (1997) A nonparametric approach to estimating divergence times in the absence of rate constancy. *Mol Biol Evol* 14:1218–1231.
7. Paradis E, Claude J, Strimmer K (2004) APE: Analyses of phylogenetics and evolution in R language. *Bioinformatics* 20:289–290.
8. Garland T, Harvey PH, Ives AR (1992) Procedures for the analysis of comparative data using phylogenetically independent contrasts. *Syst Biol* 41:18–32.
9. Legendre P, Legendre L (1998) *Numerical Ecology* (Elsevier, Amsterdam), 2nd Ed.
10. Everitt BS, Landau S, Leese M (2001) *Cluster Analysis* (Taylor & Francis, Florence, KY), 4th Ed.
11. Suzuki R, Shimodaira H (2006) Pvclust: An R package for assessing the uncertainty in hierarchical clustering. *Bioinformatics* 22:1540–1542.
12. Blomberg SP, Garland T, Jr, Ives AR (2003) Testing for phylogenetic signal in comparative data: Behavioral traits are more labile. *Evolution (Lawrence, Kans)* 57:717–745.
13. Kursar TA, Coley PD (2003) Convergence in defense syndromes of young leaves in tropical rainforests. *Biochem Syst Ecol* 21:929–949.
14. Maddison WP, Maddison DR (2007) *Mesquite: A Modular System for Evolutionary Analysis* (Mesquite Software, Austin, TX).
15. Maddison D, Maddison W (2005) *MacClade, Version 4.08* (Sinauer, Sunderland, MA).
16. Webb CO (2000) Exploring the phylogenetic structure of ecological communities: An example for rain forest trees. *Am Nat* 156:145–155.
17. Kembel SW, Hubbell SP (2006) The phylogenetic structure of a Neotropical forest tree community. *Ecology* 87:S86–S99.
18. Hardy OJ (2008) Testing the spatial phylogenetic structure of local communities: Statistical performances of different null models and test statistics on a locally neutral community. *J Ecol* 96:914–926.
19. Xie D-Y, Dixon RA (2005) Proanthocyanidin biosynthesis: Still more questions than answers? *Phytochemistry* 66:2127–2144.

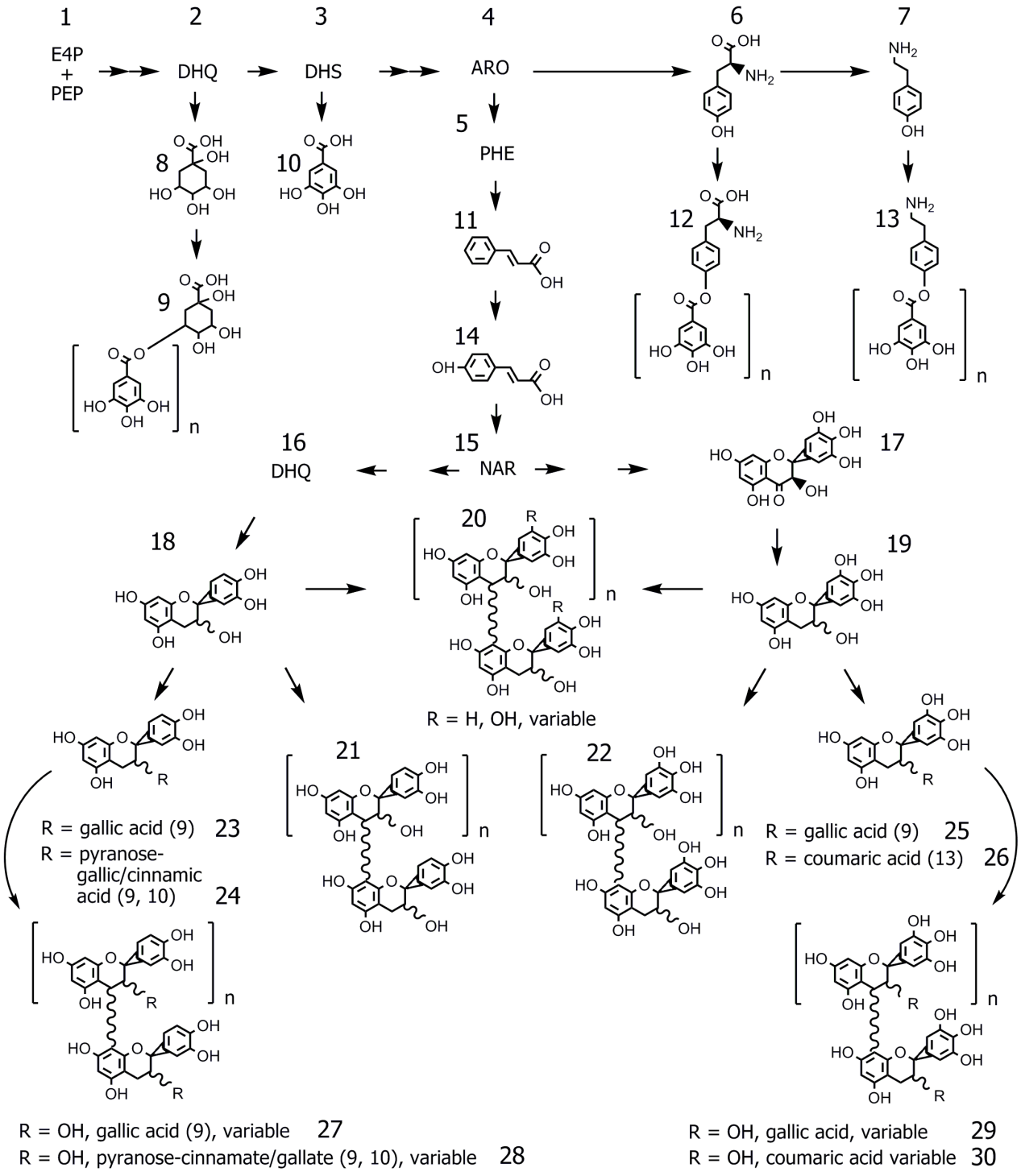

Fig. S1. Important shikimic acid/phenylpropanoid/flavonoid pathway intermediates and branch points in *Inga*. Only a subset of the biosynthetic steps are shown. The acronyms refer to biosynthetic precursors and biosynthetic intermediates. The precursors include **1**, erythrose-4-phosphate + phosphoenolpyruvate; **2**, dehydroquinic acid; **3**, dehydroshikimic acid; **4**, L-arogenate, and **5**, phenylalanine. The biosynthetic intermediates are **15**, naringenin and **16**, dihydroquercetin. The structures of the intermediate adducts, the compounds that do not accumulate to a high level in vivo as monomers but that are components of important defense metabolites, include: **7**, tyramine; **8**, quinic acid; **10**, gallic acid; **11**, cinnamic acid, and **14**, coumaric acid. The 18 end-products, the major defense metabolites that accumulate to a high level in vivo, are: **6**, tyrosine; **9**, quinic acid gallate; **12**, tyrosine gallate; **13**, tyramine gallate; **17**, dihydromyricetin; **18**, catechin/epicatechin (*c*/e); **19**, gallocatechin/galloepicatechin (gc/ge); **20**, mixed *c*/e-gc/ge polymer; **21**, *c*/e polymer; **22**, gc/ge polymer; **23**, 3-*O*-galloyl *c*/e; **24**, 3-*O*-pyrano-galloyl/cinnamoyl *c*/e; **25**, 3-*O*-galloyl gc/ge; **26**, 3-*O*-coumaroyl gc/ge; **27** and **28**, *c*/e polymer variably substituted at the 3-*O*- position; **29** and **30**. gc/ge polymer variably substituted at the 3-*O*- position. Six of the 18 listed end-products, **18**, **19**, and **23**-**26**, are also the monomeric building blocks of the indicated polymers. The other 12 end-products correspond to the 12 classes of phenolics referred to in *Results*. After Xie and Dixon (19).

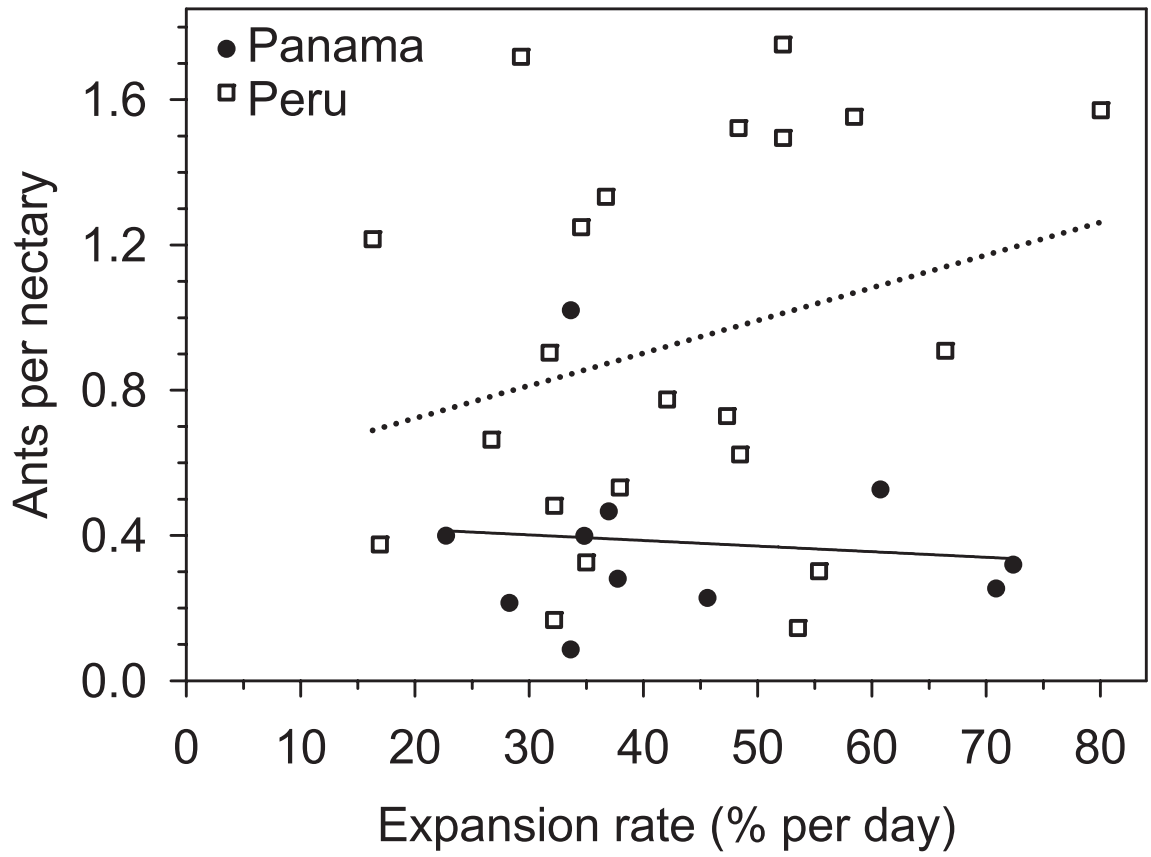

Fig. S2. The rate of expansion of young leaves expressed as the percentage increase in area per day (% per day) versus the number of ants visiting extrafloral nectaries on young leaves of *Inga* species. There was no significant relationship for either Panama (solid line, $r^2 = 0.11$, $P = 0.75$, $n = 11$) or Peru (dotted line, $r^2 = 0.069$, $P = 0.24$, $n = 22$).

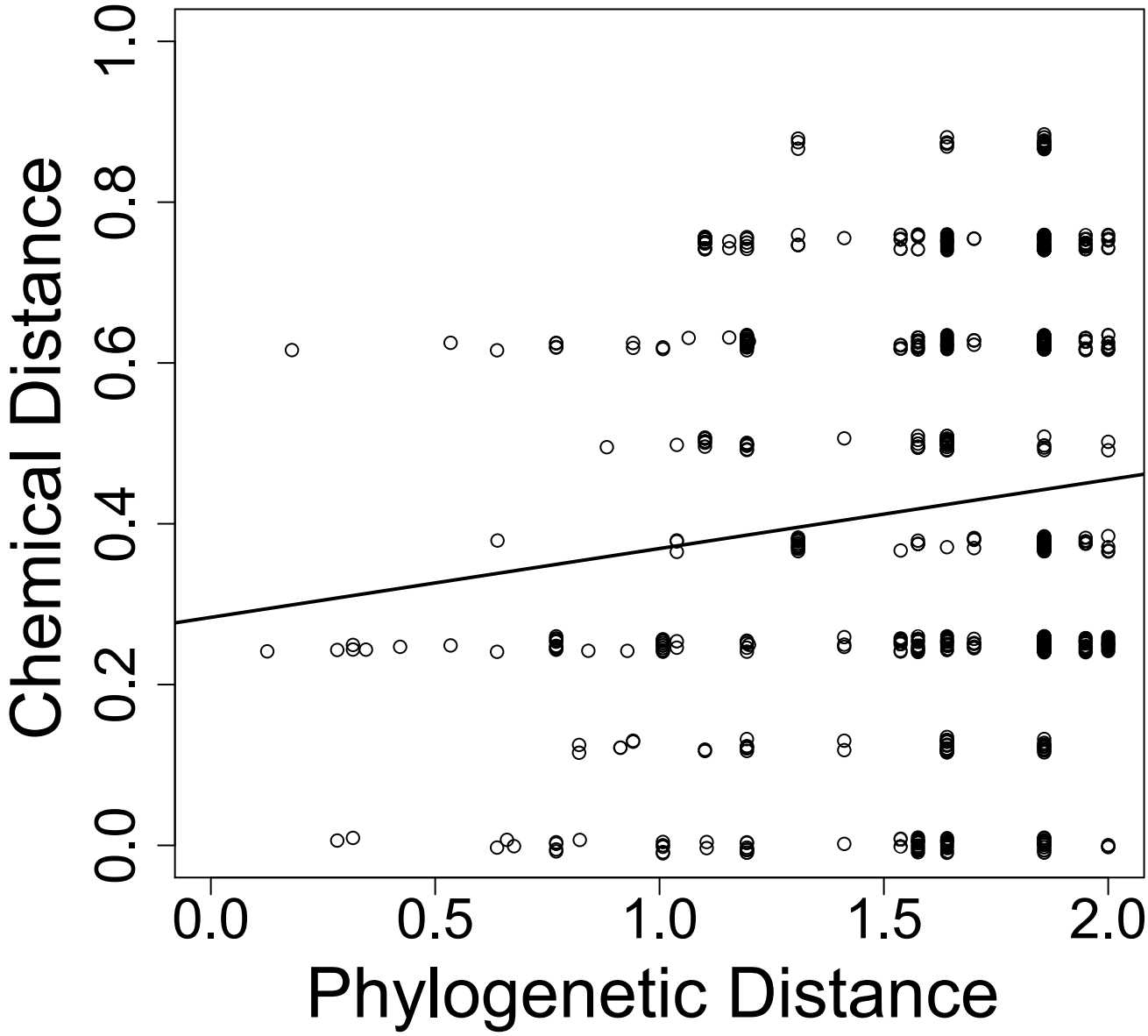

Fig. S3. Average chemical distance (weighting phenolics and saponins equally) between species by phylogenetic distance between species for one randomly selected Bayesian tree. The line represents the best-fit linear regression ($y = 0.28 + 0.086x$), while significance and fit of the relationship was evaluated by using a Mantel test (for this tree: $r = 0.12$, $P = 0.031$).

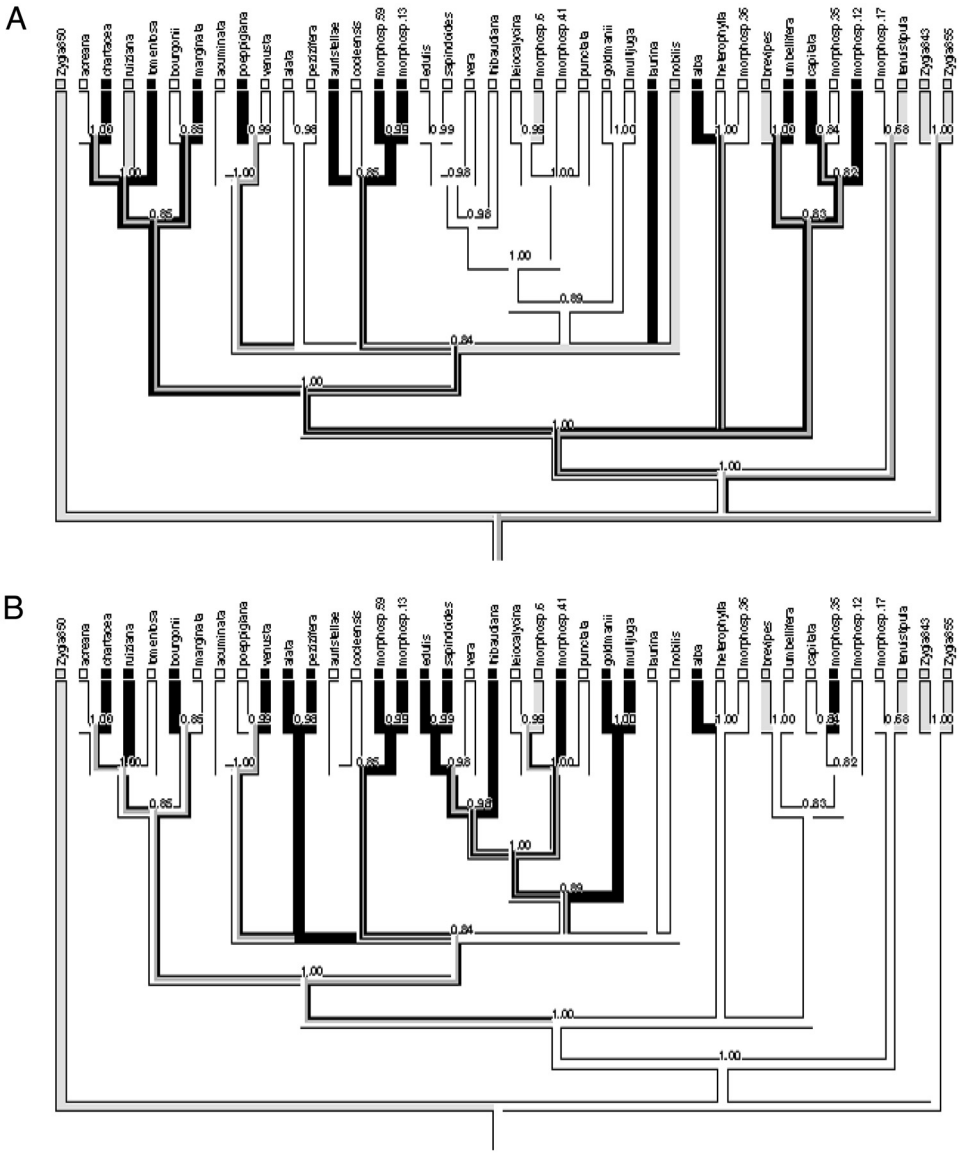

Fig. S4. Developmental and ant defense mapped onto *Inga* phylogeny. (*A*) Binary character of defense (white) and escape (black) optimized by using parsimony onto 50% majority rule Bayesian consensus tree (gray shading indicates equivocal state). Numbers adjacent to nodes are posterior probability values. To account for topological uncertainty, ancestral state reconstruction was summarized for >100 Bayesian trees sampled at stationarity, and along each branch the thickness of the line representing each state is in proportion to the number of trees in which that state is reconstructed. Low phylogenetic signal is indicated by 8–11 observed parsimony steps, which is well within the frequency distribution of the number of steps when states are randomized across terminal taxa (''reshuffle character'' option in Mesquite 2.01) (14). Furthermore, the 8–11 observed transformations lie within the frequency distribution of transformations when mapped onto 1,000 random trees generated by MacClade 4.08 (15). (*B*) Binary character of low (white) and high (black) ant visitation (gray shading indicates equivocal state) optimized using parsimony onto 50% majority rule Bayesian consensus tree. Numbers adjacent to nodes are posterior probability values. To account for topological uncertainty, ancestral state reconstruction was summarized for >100 Bayesian trees sampled at stationarity, and along each branch the thickness of the line representing each state is in proportion to the number of trees in which that state is reconstructed. Low phylogenetic signal is indicated by 10–13 observed parsimony steps, which is well within the frequency distribution of transformations when randomized across terminal taxa (reshuffle character option in Mesquite 2.01) (14). Furthermore, the 10–13 observed transformations lie within the frequency distribution of transformations when mapped onto 1,000 random trees generated by MacClade 4.08 (15).

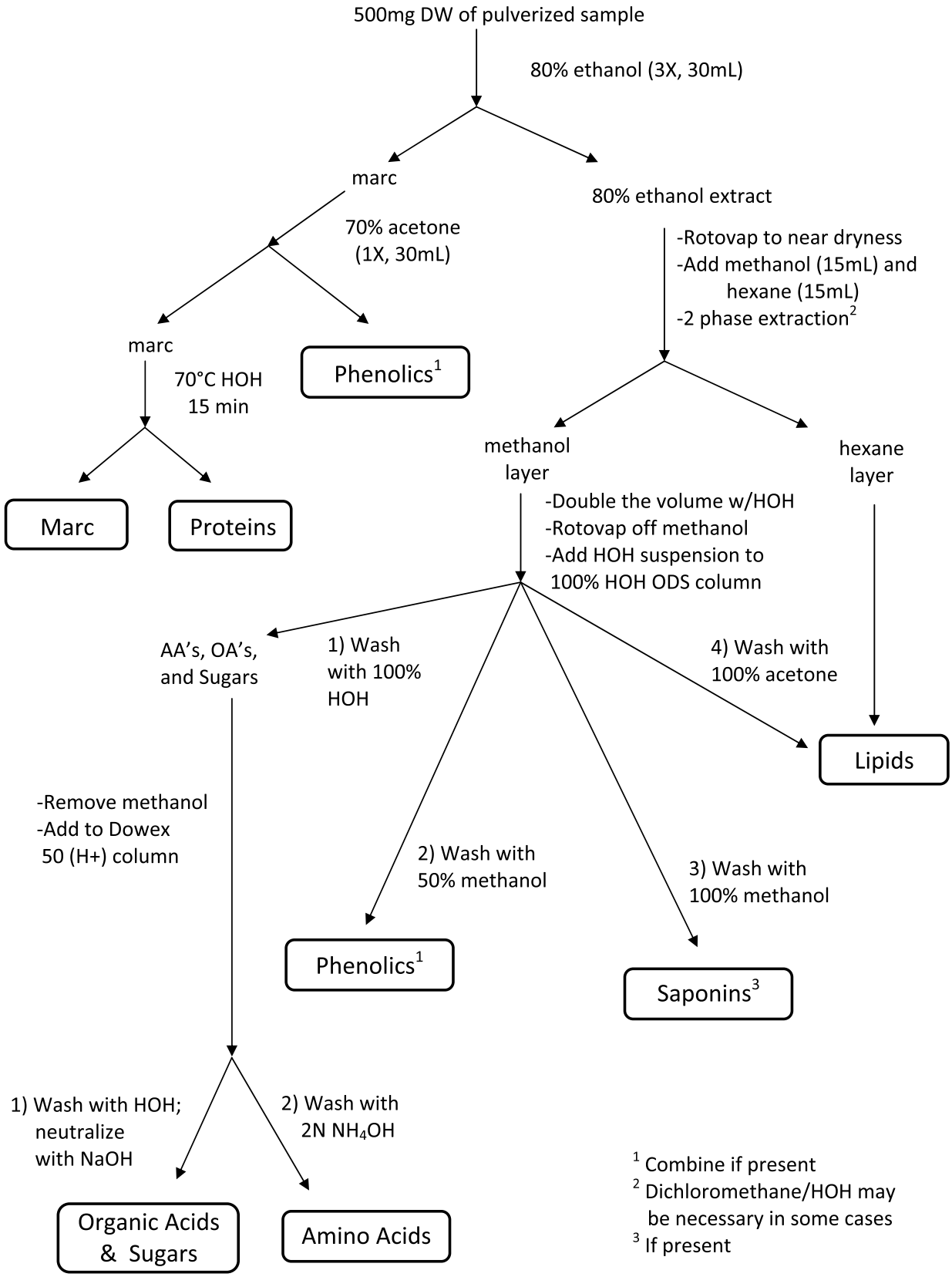

Fig. S5. The protocol used to resolve *Inga* young leaf extracts into chemically distinct fractions. The term "marc" refers to the insoluble cell walls. ODS refers to liquid chromatography on an octadecyl silane (or reversed-phase silica) column. AA, amino acids; OA, organic acids.

Table S1. Distributions of *Inga* chemotypes

Chemotype	No. of species
Phenolic/saponin	
Gallocatechin/epigallocatechin gallate	11
Saponin	5
Catechin/epicatechin	4
Gallocatechin/epigallocatechin gallate + saponin	4
Quinic acid-gallate	2
Catechin/epicatechin-methyl pyranose gallate	2
Catechin/epicatechin + saponin	2
Tyrosine gallate	2
Catechin-epicatechin gallate	1
Catechin-epicatechin-pyranose-phenolic acid + tyrosine	1
Flavone	1
Gallocatechin/epigallocatechin-gallate-coumarate + saponin	1
Tyramine gallate + quinic acid gallate	1
Amino acid	
Monohydroxypipecolic acid #2 + dihydroxypipecolic acid #2	4
5-Amino-4-hydroxypentanoic acid + *N*-methyl-hydroxyproline	1
Monohydroxypipecolic acid #3	1
Monohydroxypipecolic acid #1	1
Dihydroxypipecolic acid #4	1
Monohydroxypipecolic acid #3 + dihydroxypipecolic acid #1 + 2	1
Monohydroxypipecolic acid #3 + djenkolic acid	1
Tyrosine	1

Each chemotype is a distinct combination of metabolites. Shown are the major phenolic/saponin chemotypes for all 37 study species (Peru and Panama) and the major amino acid chemotypes for 11 study species from Panama.

Table S2. Gallocatechin/galloepicatechin gallate structures (cf. Fig. S1) inferred from MS analysis of *Cojoba arboreab* phenolic extracts and shared among 11 of the 37 *Inga* study species

Nominal mass	Gallocatechin-galloepicatechin no.	Gallate no.
458	1	1
762	2	1
914	2	2
1066	3	1
1218	3	2
1370	3	3
1370	4	1
1522	4	2
1522	5	0
1674	4	3
1674	5	1

The nominal mass refers to the actual mass, in atomic mass units, of the polymer rounded to the nearest integer. Each unit of the polymer contains either one gallocatechin or one galloepicatechin. These are identical in molecular formula and differ in stereochemistry. Therefore, the degree of polymerization is noted as gallocatechin-galloepicatechin no. The number of gallate esters is noted as gallate no. The minimum esterification with gallate is zero on the entire polymer (e.g. nominal mass 1,522, a tetramer with no gallate). The maximum esterification is one for every gallocatechin/galloepicatechin unit of the polymer (e.g. nominal mass 1,370, a trimer with three gallates). Because the table is ordered by nominal mass and because of the variation in the number of gallates per polymer, gallocatechin-galloepicatechin no. is not in numerical order. Polymers at masses in excess of the highest shown, 1,674, exist and are minor components. In the species of *Inga* characterized to date, the gallocatechin/galloepicatechins and gallic acids polymerize such that a dimer could, in principle, have eight or more forms of identical mass. Although not indicated here, we observe a subset of the possible forms of dimers, trimers, tetramers, and pentamers. These forms are distinguished as having identical masses but often distinct chromatographic behavior; they have not been fully characterized.

Table S3. Average values for the leaf traits of *Inga* species from Panama and Peru, including chlorophyll content of young leaves, rates of young-leaf expansion, and the number of ants censused at extrafloral nectaries (mean, SE, and *n*)

Inga species	Chlorophyll ($mg \cdot m^{-2}$)	Chlorophyll SE	Chlorophyll # plants	Expansion ($\% \ d^{-1}$)	Expansion SE	Expansion # plants	Escape or defense	# Ants per extrafloral nectary	Ants SE	Ants # plants	Ants-normalized	Wings on the rachis	# Leaflets per leaf
Panama													
acuminata	111	17	11	33.6	2.1	12	D	0.1	0.0	282	L	Y	12
cocleensis	89	10	11	37.7	1.8	18	D	0.3	0.0	455	L	N	14
laurina	65	5	9	70.9	2.5	11	E	0.3	0.0	139	L	N	4
goldmanii	85	5	9	33.6	0.7	18	D	1.0	0.2	219	H	Y	8
marginata	36	5	10	72.4	5.9	21	E	0.3	0.0	253	L	Y	4
multijuga	128	6	8	22.7	1.4	12	D	0.4	0.1	46	H	N	16
pezizifera	103	10	11	34.8	0.7	17	D	0.4	0.0	314	H	N	8
nobilis	49	6	13	60.7	2.8	18	E	0.5	0.2	182	H	N	8
ruiziana								0.8	0.3	5	H	N	10
sapindoides	78	7	11	36.9	1.6	15	D	0.5	0.0	275	H	Y	6
umbellifera	28	3	15	45.6	3.2	16	E	0.2	0.0	233	L	Y	6
vera	119	9	7	28.3	1.1	22	D	0.2	0.1	28	L	Y	10
Peru													
acreana	95	4	9	32.2	1.5	22	D	0.2	0.1	19	L	Y	6
alata	122	6	8	29.3	1.0	9	D	1.7	0.7	11	H	Y	12
alba	63	6	7	80.0	2.9	18	E	1.6	0.2	91	H	Y	8
auristellae	20	3	11	48.5	1.9	19	E	0.6	0.1	62	L	Y	6
bourgonii	103	7	8	52.2	2.5	7	D	1.8	0.6	21	H	Y	6
brevipes	46	2	7	58.4	2.0	8	E	1.6	0.4	12	H	Y	4
capitata	75	4	9	42.1	2.9	7	E	0.8	0.2	13	L	N	4
chartacea	63	4	8	36.7	2.5	9	E	1.3	0.3	36	H	Y	6
edulis	71	6	8	52.2	3.1	19	D	1.5	0.2	127	H	Y	8
heterophylla	61	4	8	53.5	3.1	23	D	0.1	0.0	66	L	N	8
laurina	50	4	4	55.4	2.4	2	E	0.3	0.2	6	L	N	4
leiocalycina	112	6	9	26.7	0.6	12	D	0.7	0.1	51	L	N	4
marginata							E	0.6	0.5	4	L	Y	4
morphosp.12							E					N	4
morphosp.13	66	5	10	66.4	2.2	13	E	0.9	0.1	45	H	N	6
morphosp.17	110	8	9	35.0	1.8	10	D	0.3	0.2	23	L	N	8
morphosp.35	90	4	7	16.3	1.6	6	D	1.2	0.4	48	H	N	4
morphosp.36	74	8	3				D	0.1	0.0	8	L	N	12
morphosp.41	107	7	7	31.8	1.0	6	D	0.9	0.4	8	H	N	8
morphosp.59	70	2	10	48.3	3.2	10	E	1.5	0.5	26	H	N	4
morphosp.6								0.4	0.3	6	L	N	4
nobilis								0.6	0.5	5	L	N	14
poeppigiana	56	6	12	32.2	2.0	14	E	0.5	0.1	42	L	Y	6
punctata				19.7	0.4	2	D	0.7	0.3	4	L	N	4
ruiziana	79	4	5					0.4	0.5	3	L	N	8
tenuistipula	151	26	3	16.9	0.3	2	D	0.4	0.2	8	L	N	6
thibaudiana	120	14	8	34.5	1.9	15	D	1.2	0.2	124	H	N	12
tomentosa	84	6	7	47.3	1.9	26	E	0.7	0.2	39	L	Y	6
umbellifera	40	5	8	37.9	2.6	6	E	0.5	0.1	27	L	Y	4
venusta	156	19	7	21.4	3.9	6	D	9.5	5.1	23	H	Y	6

Developmental strategies of escape or defense were assigned based on chlorophyll and expansion (see Fig. 2). Because ant visitation was different between sites, we characterized the numbers of ants at nectaries as high (H) if they were above the site average or low (L) if they were below the site average. The presence or absence of wings on the rachis and the number of leaflets per leaf were determined for saplings in the field.

Table S4. Collection details and GenBank accession numbers of material used for phylogenetic study

Taxon	Voucher details	Country	Locality	Herbarium	GenBank accession nos.					
					trnL-trnF	*trnD-trnT*	*trnH-psbA*	*rps16*	*rpoC1*	*ndhF-rpl32*
Zygia 843	Kyle Dexter 843	Peru	Madre de Dios	Duke	GQ118709	FJ974145	GQ118858	GQ118826	GQ118787	GQ118748
Zygia 850	Kyle Dexter 850	Peru	Madre de Dios	Duke	GQ118710	FJ974151	GQ118859	GQ118827	GQ118788	GQ118749
Zygia 855	Kyle Dexter 855	Peru	Madreselva, Loreto	Duke	GQ118711	GQ871278	GQ118860	GQ118828	GQ118789	GQ118750
Inga acreana Harms	Kyle Dexter 390	Peru	Madre de Dios, Los Amigos	Duke	GQ118712	FJ974164	GQ118861	GQ118829	GQ118790	GQ118751
Inga acuminata Benth.	Thomas Kursar & Phyllis Coley 1266	Panama	Barro Colorado Island	K, STRI	GQ118713	GQ871263	GQ118862	GQ118830	GQ118791	GQ118752
Inga alata Benoist	Kyle Dexter 402	Peru	Madre de Dios, Los Amigos	K	GQ118714	FJ974180	GQ118863	GQ118831	GQ118792	GQ118753
Inga alba (Sw.)Willd.	Kyle Dexter 494	Peru	Madre de Dios, Los Amigos	K	GQ118715	FJ974241	GQ118864	GQ118832	GQ118793	GQ118754
Inga auristellae Harms	Kyle Dexter 10	Peru	Madre de Dios, Los Amigos	K	GQ118716	FJ974279	GQ118865	GQ118833	GQ118794	GQ118755
Inga bourgonii (Aubl.)DC.	Kyle Dexter 404	Peru	Madre de Dios, Los Amigos	K	GQ118717	FJ974351	GQ118866	GQ118834	GQ118795	GQ118756
Inga brevipes Benth.	Kyle Dexter 202	Peru	Madre de Dios, Los Amigos	K	GQ118718	FJ974409	GQ118867	-	GQ118796	GQ118757
Inga capitata Desv.	Thomas Kursar & Phyllis Coley 1568	Peru	Madre de Dios, Los Amigos	MOL	GQ118719	GQ871264	-	GQ118835	GQ118797	GQ118758
Inga chartacea Poepp. & Endl.	Kyle Dexter 358	Peru	Madre de Dios, Los Amigos	K	GQ118720	FJ974449	GQ118868	GQ118836	GQ118798	GQ118759
Inga cocleensis Pittier	Thomas Kursar & Phyllis Coley 1273	Panama	Barro Colorado Island	K, STRI	GQ118721	GQ871265	GQ118869	GQ118837	GQ118799	GQ118760
Inga edulis Mart.	Kyle Dexter 386	Peru	Madre de Dios, Los Amigos	K	GQ118722	FJ974509	GQ118870	GQ118838	GQ118800	GQ118761
Inga goldmanii Pittier	Thomas Kursar & Phyllis Coley 1271	Panama	Barro Colorado Island	K, STRI	GQ118723	GQ871266	GQ118871	GQ118839	GQ118801	GQ118762
Inga heterophylla Willd.	Thomas Kursar & Phyllis Coley 1528	Peru	Madre de Dios, Los Amigos	MOL	GQ118724	GQ871267	-	-	GQ118802	-
Inga morphosp.36	Thomas Kursar & Phyllis Coley 1545	Peru	Madre de Dios, Los Amigos	MOL	GQ118725	GQ871268	-	-	GQ118803	GQ118763
Inga morphosp.59	Thomas Kursar & Phyllis Coley 1635	Peru	Madre de Dios, Los Amigos	MOL	GQ118726	GQ871269	GQ118872	-	GQ118804	GQ118764
Inga leiocalycina Benth.	Thomas Kursar & Phyllis Coley 1593	Peru	Madre de Dios, Los Amigos	MOL	GQ118727	GQ871270	-	-	GQ118805	GQ118765
Inga marginata Willd.	Kyle Dexter 463	Peru	Madre de Dios, Los Amigos	K	GQ118728	FJ974628	GQ118873	GQ118840	GQ118806	GQ118766
Inga morphosp.13	Kyle Dexter 29	Peru	Madre de Dios, Los Amigos	K	GQ118729	FJ974988	GQ118874	GQ118841	GQ118807	GQ118767
Inga morphosp.41	Kyle Dexter 37	Peru	Madre de Dios, Los Amigos	K	GQ118730	FJ975003	GQ118875	GQ118842	GQ118808	GQ118768
Inga morphosp.17	Kyle Dexter 53	Peru	Madre de Dios, Los Amigos	K	GQ118731	FJ975011	GQ118876	GQ118843	GQ118809	GQ118769
Inga morphosp.12	Kyle Dexter 349	Peru	Madre de Dios, Los Amigos	K	-	FJ974438	-	-	GQ118810	GQ118770
Inga laurina (Sw.)Willd.	Kyle Dexter 526	Peru	Madre de Dios, Los Amigos	Duke	GQ118732	FJ975039	GQ118877	GQ118844	GQ118811	GQ118771
Inga multijuga Benth.	Thomas Kursar & Phyllis Coley 1274	Panama	Barro Colorado Island	K, STRI	GQ118733	GQ871271	GQ118878	GQ118845	GQ118812	GQ118772
Inga nobilis Willd.	Kyle Dexter 163	Peru	Madre de Dios, Los Amigos	K	GQ118734	FJ974673	GQ118879	GQ118846	GQ118813	GQ118773
Inga pezizifera Benth.	Thomas Kursar & Phyllis Coley 1001	Panama	Barro Colorado Island	K, STRI	GQ118735	GQ871272	GQ118880	GQ118847	GQ118814	GQ118774
Inga poeppigiana Benth.	Kyle Dexter 85	Peru	Madre de Dios, Los Amigos	K	GQ118736	FJ974683	GQ118881	GQ118848	-	GQ118775
Inga punctata Willd.	Kyle Dexter 475	Peru	Madre de Dios, Los Amigos	K	GQ118737	FJ974713	GQ118882	GQ118849	GQ118815	GQ118776
Inga ruiziana G.Don	Thomas Kursar & Phyllis Coley 1256	Panama	Barro Colorado Island	K, STRI	GQ118738	GQ871273	GQ118883	GQ118850	GQ118816	GQ118777
Inga sapindoides Willd.	Thomas Kursar & Phyllis Coley 1264	Panama	Barro Colorado Island	K, STRI	GQ118739	GQ871274	GQ118884	GQ118851	GQ118817	GQ118778
Inga morphosp.6	Thomas Kursar & Phyllis Coley 1561	Peru	Madre de Dios, Los Amigos	MOL	GQ118740	GQ871275	-	-	GQ118818	GQ118779
Inga morphosp.35	Thomas Kursar & Phyllis Coley 1560	Peru	Madre de Dios, Los Amigos	MOL	GQ118741	GQ892055	-	-	GQ118819	GQ118780
Inga tenuistipula Ducke	Kyle Dexter 110	Peru	Madre de Dios, Los Amigos	K	GQ118742	FJ974870	GQ118885	GQ118852	GQ118820	GQ118781
Inga thibaudiana DC.	Kyle Dexter 340	Peru	Madre de Dios, Los Amigos	K	GQ118743	FJ974883	GQ118886	GQ118853	GQ118821	GQ118782
Inga tomentosa Benth.	Kyle Dexter 102	Peru	Madre de Dios, Los Amigos	K	GQ118744	FJ974910	GQ118887	GQ118854	GQ118822	GQ118783
Inga umbellifera (Vahl)Steud.	Thomas Kursar & Phyllis Coley 1318 (collected by S Ring and B Wolfe)	Panama	Barro Colorado Island	K, STRI	GQ118745	GQ871276	GQ118888	GQ118855	GQ118823	GQ118784

Taxon	Voucher details	Country	Locality	Herbarium	GenBank accession nos.					
					trnL-trnF	*trnD-trnT*	*trnH-psbA*	*rps16*	*rpoC1*	*ndhF-rpl32*
Inga venusta Standl.	Kyle Dexter 78	Peru	Madre de Dios, Los Amigos	K	GQ118746	FJ974975	GQ118889	GQ118856	GQ118824	GQ118785
Inga vera Willd.	Thomas Kursar & Phyllis Coley 1308 (collected by D Dvorett and S Ring)	Panama	Barro Colorado Island	K, STRI	GQ118747	GQ871277	GQ118890	GQ118857	GQ118825	GQ118786

Duke, Duke University, Durham, NC; K, Royal Botanic Gardens, Kew, United Kingdom; STRI, Smithsonian Tropical Research Institute, Balboa, Panama; MOL, Universidad Nacional Agraria, La Molina, Lima, Peru. Dash indicates no sequence was obtained.